# The SiD Digital ECal Based on Monolithic Active Pixel Sensors

*James E.* Brau[1,*], *Martin* Breidenbach[2], *Angelo* Dragone[2], *Alexandre* Habib[2], *Lorenzo* Rota[2], *Mirella* Vassilev[2], and *Caterina* Vernieri[2,**]

[1]University of Oregon, Eugene, OR USA
[2]SLAC National Accelerator Laboratory, Menlo Park, CA, USA

**Abstract.** Higgs physics goals with detectors at future colliders demand unprecedented precision. Linear colliders, with energy reach to the TeV scale and low duty cycles and backgrounds, enable this high precision performance. The SiD Collaboration is developing Monolithic Active Pixel Sensor (MAPS) technology for tracking and electromagnetic calorimetry (ECal). This technology offers high granularity, thin sensors, good time resolution (<nsec), and small dead areas, enabled by gaseous cooling for tracking and passive thermal conduction for calorimetry. The first MAPS prototype (NAPA-p1), designed by SLAC in CMOS imaging 65 nm technology, is under test. The long-term objective is a wafer-scale sensor of area $5 \times 20$ cm$^2$. Detailed simulation of ECal performance confirms previous results, indicating electromagnetic energy resolution based on digital hit cluster counting provides better performance than the 13 mm$^2$ pixels SiD TDR analog design, and two particle separation in the ECal is excellent down to the millimeter scale. Recent heat management analysis indicates passive cooling for the low duty cycle linear colliders should work.

## 1 Introduction

Recent work on application of Monolithic Active Pixels (MAPS) for the Higgs factory experiments promises to contribute to the required high performance of those experiments. The Higgs factory is widely recognized as the next step toward fully revealing the role of the Higgs boson in the fundamental nature of the universe [1, 2]. Unprecedented precision is needed to address the Higgs physics with detectors at these future $e^+e^-$ colliders [3]. The Higgs factory measurements will benefit from low backgrounds relative to, for example, the Large Hadron Collider, and the linear colliders (such as ILC, $C^3$, and CLIC) will operate with low duty cycles based on the timing structures shown in Figure 2; these conditions enable detector concepts to achieve the very high precision detector performance goals, with reach to the TeV center-of-mass energy. Capitalizing on these conditions, the SiD Collaboration [4] is developing an application of Monolithic Active Pixel Sensor (MAPS) technology for its tracking and electromagnetic calorimetry (ECal). A schematic cross section of the optimized sensor design is illustrated in Figure 1. The ionization left by the passage of a charged particle through the high resistivity, epitaxial layer of $\sim$10 $\mu$m is collected by the readout electronics.

*e-mail: jimbrau@uoregon.edu
**e-mail: caterina@slac.stanford.edu

This technology offers high granularity, thin sensors, fast responses (<nsec), and small dead areas. The low linear collider duty cycle enables gaseous cooling for the tracker and passive heat removal for the calorimeter.

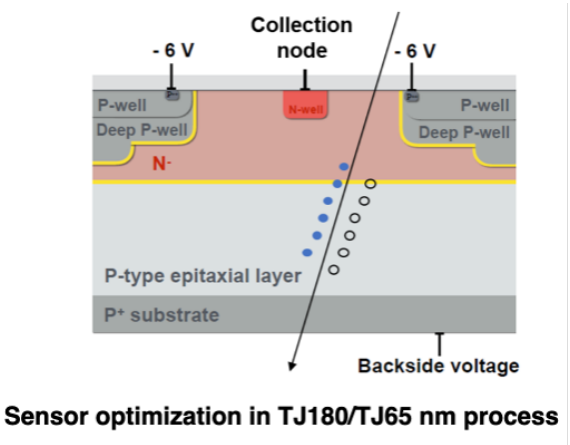


**Figure 1.** Schematic cross section of sensor optimized in TJ180/TJ65 nm process


**Figure 2.** Linear Collider Timing Structure

## 2 The prototype sensor: NAPA-p1

The first MAPS prototype of this effort (NAPA-p1, NAnosecond timing Pixel for large Area sensors — prototype1), designed by SLAC in CMOS imaging 65 nm technology, has been produced and is now under test [5](illustrated in Figure 3). Simulations of the concept predict a pixel jitter of $< 400$ ps-rms and an equivalent noise charge of 13 $e^-$rms with an average power consumption of 1.15 mW/cm$^2$ assuming a 1% duty cycle enabled by the linear collider. The prototype has dimensions of 1.5 mm $\times$ 1.5 mm and a pixel pitch of 25 $\mu$m. The long-term objective is to develop a wafer-scale sensor with an area $\sim$ 5 cm $\times$ 20 cm. Application of large area MAPS in these systems eliminates delicate and expensive bump-bonding, provides possibilities for better timing, and uses a CMOS foundry process.

## 3 SiD and its electromagnetic calorimeter (ECal)

SiD (Figure 4) has been designed to make precision measurements of the Higgs boson, W- and Z-boson, the top quark and other particles at the linear collider [4]. With relatively benign

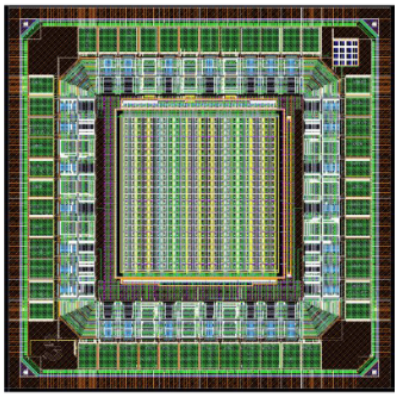


**Figure 3.** Layout of SLAC prototype for WP1.2 2022 shared submission on TowerSemi 65nm

linear collider experimental conditions, the detector can be optimized for these precision measurements. There are lower collision rates, lower complexity, and less background than experienced in a hadron collider.

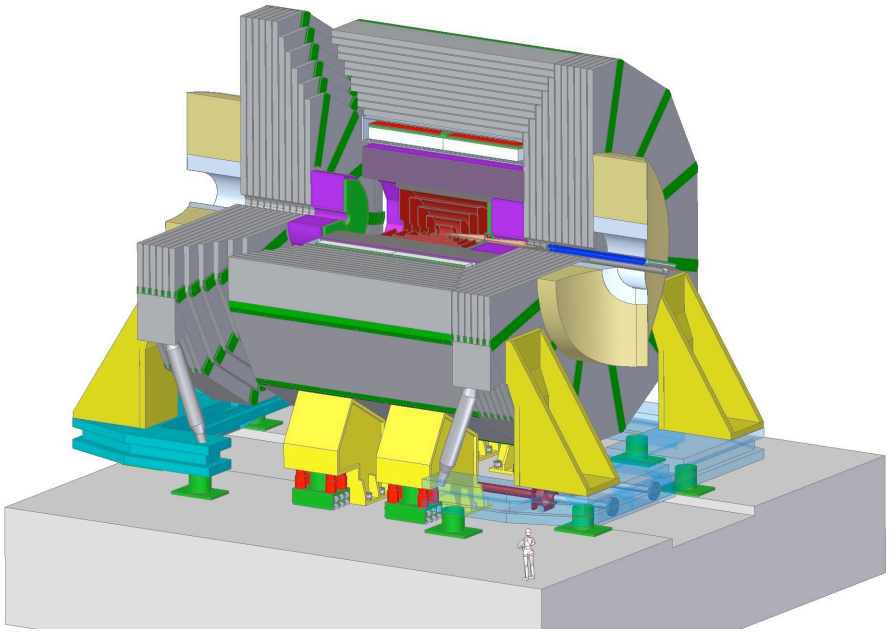

**Figure 4.** SiD on its platform, showing tracking (red), ECAL (light green), HCAL (violet) and do-decagonal iron yoke

.

The requirements in calorimetry performance are driven by excellent jet reconstruction and measurement. Detection and separation of W and Z bosons in their hadronic decay modes

is essential, and this motivates application of a PFA and a goal of 3–4% jet mass resolution at energies above 100 GeV, about twice as good as achieved in hadron collisions at the LHC.

In the new MAPS ECal concept, the longitudinal structure of the SiD ECal defined in the ILC TDR [6] remains unchanged. The ECal has thirty total layers (Figure 5). The first twenty layers each have 2.5 mm tungsten thickness and 1.25 mm readout gap. The last ten layers each have 5 mm tungsten plus the same 1.25 mm readout gap. The total depth is 26 radiation lengths, providing reasonable containment for high-energy showers.

In order to preserve the 14 mm Moliere radius of the calorimeter with the 1.25 mm readout gap, power pulsing and passive cooling is used. For this, the power pulsing enabled by the linear collider time structure (Figure 2) is essential. One end of each ECal wedge provides a cold plate and the heat is conducted from the sampling layers through the tungsten layers to the cold plate. For the sparsest time structure of $C^3$ this leads to a maximum temperature rise of 2 K at the far corner of the module, and a rise of 16 K for ILC operation which has beam bunching with a higher duty cycle of 0.5%. Figure 6 presents an estimate of the temperature rise throughout the barrel module for the ILC bunch train. Colliders that operate with higher duty cycles up to 100% will require active cooling.

A 25 $\mu$m × 100 $\mu$m pixel geometry of the 2500 $\mu m^2$ area was initially chosen for the tracking precision from the 25 $\mu$m size in the bend plane and used with the same configuration for the ECal. Recent tracking considerations have led to a favoring of 25 $\mu$m × 50 $\mu$m

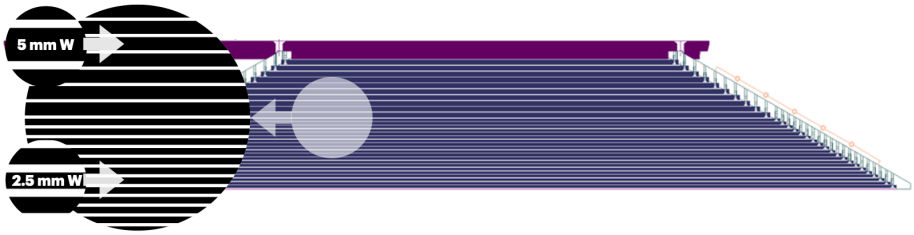


**Figure 5.** SiD ECal barrel wedge. Each wedge is built of twenty "thin and longer" layers (2.5 mm thick tungsten and a 1.25 mm gap containing the MAPS sensors) followed by ten "thick and shorter" layers (5 mm thick tungsten and a 1.25 mm gap with sensors). The SiD ECal is composted of twelve overlapping wedges without projective cracks, surrounded and mounted on the hadron calorimeter. The front layer of the hadron calorimeter is shown at the top of the image

.

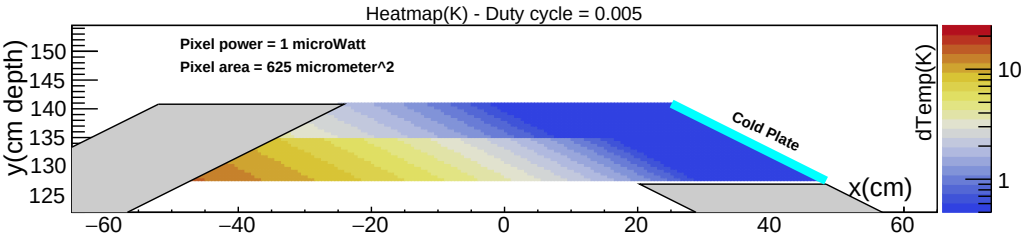


**Figure 6.** Heat map of the SiD ECal barrel wedge for the 0.5% duty cycle of the ILC bunch train power pulsing. The smaller pixel size of 25 $\mu$m × 25 $\mu$m is assumed, operating with the ILC duty cycle. For the lower duty cycle of $C^3$ or CLIC the heat rise is even smaller.

or 25 $\mu$m, but the earlier segmentation is used in these studies. Excellent performance with a purely digital ECal based on this fine granularity is expected given the spreading of the electromagnetic showers and the consequent number of pixels activated. A 25 $\mu$m $\times$ 100 $\mu$m pixel geometry is found to achieve ECal performance equivalent to 50 $\mu$m $\times$ 50 $\mu$m. Studies [8–10] have shown potential energy resolution advantages for a digital ECal application and were referenced in the ILC TDR. The prototype of a similar concept was beam tested and has been published [11].

The MAPS design for SiD's ECal and tracking sensors requires 1364 $m^2$ of silicon, including 54 $m^2$ in the barrel tracker, 20 $m^2$ in the end cap tracker, 1000 $m^2$ in the barrel ECal, and 290 $m^2$ in the end cap ECal. The readout is sparse, involving a very small fraction of the pixels and occurring in the period between bunch trains. There is no trigger.

## 4 Performance

GEANT4 simulation studies based on this fine digital configuration confirmed the previous MAPS studies referred to in the ILC TDR and demonstrated additional details on the performance, including better energy resolution than that of the SiD TDR analog design based on 13 $mm^2$ pixels [12]. This results from the large number of MAPS pixels, with the specified granularity, active in electromagnetic showers. While aimed at understanding the ultimate performance and limitations of the digital ECal, the simulation studies also inform the ASIC designers on the requirements for the sensor chips. These studies compare the electromagnetic energy resolution based on counting clusters of hits in the MAPS sensors, and weighting them based on longitudinal and transverse position in shower, with the analog measurements provided by the much smaller number of 13 $mm^2$ TDR design pixels. The 5 Tesla magnetic field of SiD required by the tracking was found to have a minor effect, degrading the resolution by a few per cent due to the field's impact on the lower energy electrons and positrons in a shower. The small pixels also significantly improve shower separation in the ECal, an important feature for hadron shower measurements with the particle flow technique, with showers and particle distinguishable down to the millimeter scale.

One advantage of this digital approach over the TDR analog approach is the reduction in effects due to variations in energy deposition, such as Landau fluctuations. Fluctuations in the development of the shower remain as the main contribution to resolution. The fine granularity also reduces the likelihood of overlapping particles per pixel and improves the separation of nearby distinct showers, such as from high-energy $\pi^0$s or jets, and contributes to improved particle flow pattern recognition. The nature of these effects has been quantified with the GEANT4 simulations.

The excellent separation of two showers is shown in Figure 7 for two 20 GeV gamma showers from a 40 GeV $\pi^0$ decay. The fine granularity of pixels provides excellent separation, with identification of two showers down to the mm scale of separation; the energy resolution of each of the showers does not degrade significantly for the mm scale of shower separation.

While easily matching the energy measurement and consequential resolution of the larger, analog structure in the TDR pixel design, the measurement in the finely granular MAPS can be optimized. To understand this, we have begun by comparing the number of pixels with energy deposition in the 12 $\mu$m of sensitive epitaxial layer above the threshold of about 1/4 MIP (MIP $\sim$4 keV , including integration over angles of incidence), or 1 keV, and the number of particles with kinetic energies over 0.1 MeV passing through the sensors. These two counts are referred to as Hits and MIPs. For example, 20 GeV gammas in the SiD 5 Tesla field produce mean values of about 2500 Hits and 1400 MIPs. The increase in Hits over MIPs results from energy deposition by electrons and positron with kinetic energy below the 0.1 MeV MIP threshold, delta ray production, gamma absorption, and pixel charge sharing

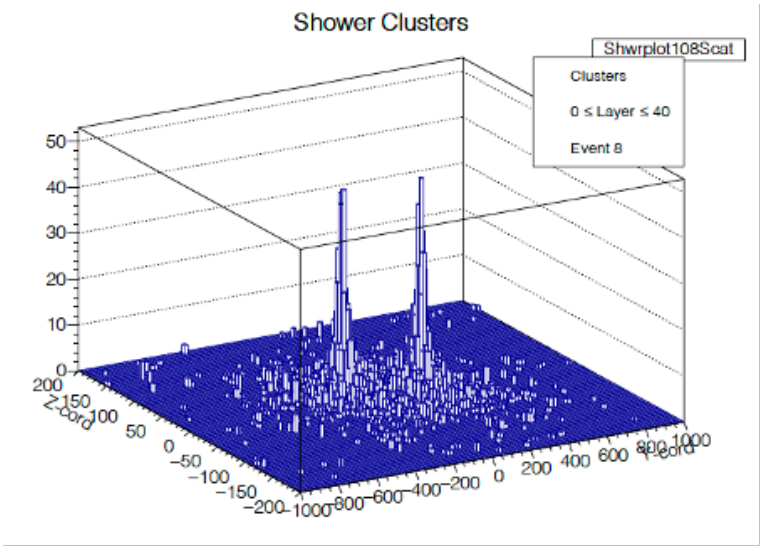


**Figure 7.** Display of clusters from 40 GeV $\pi^0 \rightarrow$ two 20 GeV $\gamma$'s separated by 10 mm

for MIPs. The MIP count represents an ideal, potential signal, while the Hit count is the simplest measurement, without optimization considerations of the shower and hit properties. For the 20 GeV gammas, the resolutions are 4.2% and 2.0%. However, the properties of the digital Hit distributions can be used to improve the experimental resolution. The noise from electronics is ignored, but is not expected to significantly affect results.

The MIPS performance described above refers to all MIPS passing through the silicon (shown as "ALL mips" in Figure 8) ignoring the finite pixel size and the loss of resolution that results from the pile up mips in a single pixel (shown as "mip active pixels" in Figure 8). At 20 GeV, when multiple mips in the same pixel are counted just once, the GEANT4 simulations reduce the count of MIPS to about 1250 at 20 GeV and degrades the MIPS resolution to about 2.5%. This is still significantly better than the Hits performance. It is notable in Figure 8 that the pileup of mips along the axis of the shower that results in increased loss of discrimination of multiple particles affects scaled energy performance at higher energy.

The MIPs performance sets an idealized goal for the experimental resolution; an algorithm of the Hits which reaches as closely as possible this assumed ideal performance is sought. An initial improvement is achieved by combining Hits into clusters and counting clusters. A cluster is constructed by combining all Hits that touch each other on any of the eight connections, boundaries or corners. An additional improvement comes from noting the probability that multiple MIPs appear in clusters as a function of the cluster size and the cluster position in the shower, longitudinally and transversely. By applying both of these corrections, the 20 GeV gamma resolution is brought to 3.3%. The resulting energy-dependent resolution between 1 and 50 GeV is well characterized by $12.2\%/\sqrt{E} \oplus 1.4\%$, compared to the MIP resolution of $9.8\%/\sqrt{E} \oplus 1.1\%$.

Figure 8 shows the gamma energy resolution performance for the range of measurements from the basic MIP counting (light blue, an idealized, best possible resolution) to that achieved by analyzing Hits in clusters (dark blue). These simulations are now mature and are well positioned to guide the design and production of the sensors. Future studies will include optimized shower reconstruction and $\pi^0$s within jets, electromagnetic shower sepa-

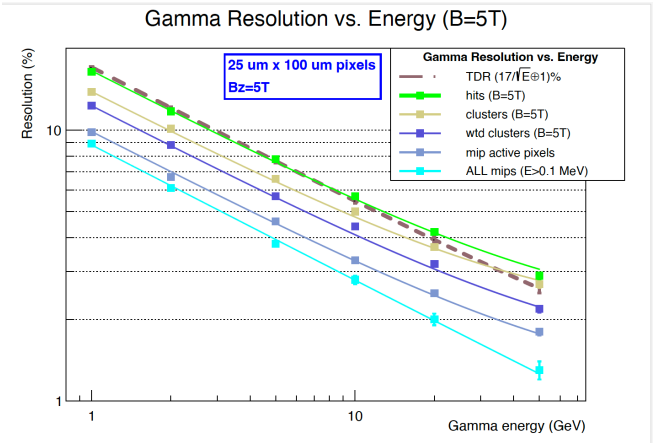


**Figure 8.** Energy resolution for gamma showers vs. energy:
ALL mips: 8.8%/ $\sqrt{E} \oplus 0.2\%$;
mips ac pix: 9.8%/ $\sqrt{E} \oplus 1.1\%$;
wtd clusters: 12.2%/ $\sqrt{E} \oplus 1.4\%$;
clusters 13.7%/ $\sqrt{E} \oplus 1.9\%$;
Hits 16.4%/ $\sqrt{E} \oplus 2.0\%$;
TDR 17%/ $\sqrt{E} \oplus 1.0\%$.

ration from other depositions in the ECal, and the impact of each on jet energy resolution, particularly for Higgs branching ratio measurements. The large volume of data provided by a MAPS-based ECal reveals details of particle showers. The extraction of the most pertinent information, e.g., particle energy, particle type, and the separation of nearby and overlapping showers, provides an opportunity to apply Machine Learning techniques. We have begun an application of such learning methods to particle and jet reconstruction in the SiD collider detector ECal based on MAPS technology.

The future work studies will include:

- Potential of multi-bit digital operation;
- Jet reconstruction, including machine learning applications;
- Mechanical design of modules including heat removal;
- Optimization of the overall ECal design, including consideration of manufacturability, possible with robots.

## 5 Conclusion

The SiD tracking and ECal systems based on MAPS will achieve significantly improved performance from that envisioned in the ILC TDR [6]. The SiD MAPS development particularly improves speed and resolution performance. The application will enable large scale use of MAPS at a reasonable cost, which benefits future colliders in general that need large areas of silicon sensors, O(1000) $m^2$, for low mass trackers and sampling calorimetry. The requirements for trackers and calorimeters, particularly very thin, large areas with micron scale resolution, are driving this work. The low duty cycle of linear colliders allow operation timed with the accelerator bunch train, with power reduced by more than two orders of magnitude by powering off analog front-end circuitry during dead-time between bunch trains. The pixel front-end circuitry is being designed to allow this power pulsing with the synchronous readout architecture so the noise and timing performance of the circuitry can be optimized while maintaining low-power consumption. The development of wafer-scale MAPS will allow designers to investigate and optimize the power pulsing, power distribution, yield, stitching techniques, assembly and power delivery.

The authors were supported by the U.S. Department of Energy contract DE-AC03-76SF00515 and grant DE-SC0017996 for this research.

## References


[1] "Exploring the Quantum Universe; Pathways to Innovation and Discovery in Particle Physics - Report of the 2023 Particle Physics Project Prioritization Panel". US Particle Physics.
https://www.usparticlephysics.org/2023-p5-report/

[2] "2020 Update of the European Strategy for Particle Physics,"
https://home.cern/sites/default/files/2020-06/2020

[3] "The International Linear Collider: Report to Snowmass 2021," arXiv:2203.07622 [physics.acc-ph]

[4] https://pages.uoregon.edu/silicondetector/; silicondetector.org

[5] Habib, A.; et al. "NAPA-p1: monolithic nanosecond timing pixel for large area sensors, designed for future $e^+e^-$ colliders," JINST 19 (2024) 04, C04033.

[6] Behnke, T.; et al., "The International Linear Collider Technical Design Report - Volume 4: Detectors," arXIV:1306.6329[physics.ins-det].

[7] Apresyan, A.; et al. "Detector R&D needs for the next generation $e^+e^-$ collider," arXiv:2306.13567 [hep-ex].

[8] Ballin, J.A.; et al. "A Digital ECAL based on MAPS," arXiv:0901.4457.

[9] Stanitzki, M.; SPiDeR Collaboration. "Advanced monolithic active pixel sensors for tracking, vertexing and calorimetry with full CMOS capability," *Nucl. Instrum. Methods Phys. Res. Sect. A Accel. Spectrometers Detect. Assoc. Equip.* **2011**, *650*, 178–183.

[10] Dauncey P.; SPiDeR Collaboration. "Performance of CMOS sensors for a digital electromagnetic calorimeter," *PoS* **2010**, *502*, ICHEP2010.

[11] De Haas, A.P.; et al. "The FoCal prototype—An extremely fine-grained electromagnetic calorimeter using CMOS pixel sensors," *J. Instrum.* **2018**, *13*, P01014.

[12] Steinhebel, A.; Brau, J. “Studies of the Response of the SiD Silicon-Tungsten ECal,” SLAC-econf-C161205.4. arXiv:1703.08605 [physics.ins-det].